３次元オイラー方程式を用いた Waverider 周りの流れシミュレーション

Flow Simulation of a Waverider Using the Three-Dimensional Euler Equations

ロビア・マーカス （東大工院）、鈴木宏二郎 （東大新領域）
Marcus Lobbia, Kojiro Suzuki
E-mail: mlobbia@hotmail.com, suzuki@kl.t.u-tokyo.ac.jp
〒113-8656 東京都文京区本郷 7-3-1
Dept. of Aeronautics and Astronautics, Univ. of Tokyo, Hongo 7-3-1, Bunkyo-ku, Tokyo, 113-8656 JAPAN

Waveriders are supersonic or hypersonic vehicles that have an attached shock wave along their leading edge. Because there is no leakage of the lower surface flow into the upper surface flowfield, they have the potential to attain high lift/drag (L/D) ratios. A Mach 3.5 waverider has been designed from a supersonic conical flowfield; through the use of CFD, numerical validation of this design is performed. The three-dimensional Euler equations are solved around the waverider; these results are then compared with the analytical results used during the design process. Prelminary results from a coarse grid solution show close agreement in the performance characteristics of the waverider (C_L, C_D, L/D), although some leakage of the lower surface flow was evident near the leading edges of the design.

１．INTRODUCTION

1.1 High-Speed Aerospace Vehicle Design

For high-speed aerospace vehicles, a high lift/drag ratio (L/D) is essential for efficient operation. This allows lower-cost operation of the vehicle, thus making more realistic an array of potential applications (e.g., spaceplane, supersonic/hypersonic cruise vehicles).

Taking a closer look at the example of a supersonic or hypersonic cruise vehicle, the benefits of increasing the L/D of the design can be seen from the Breguet equation for cruise range:

$$ln\left(\frac{m_f + m_s}{m_s}\right) = d\left(\frac{SFC}{U}\right)\left(\frac{1}{L/D}\right), \qquad (1)$$

where m_f is the total fuel mass, m_s is the mass of the vehicle structure and payload (not including fuel), d is the cruise range, SFC is the specific fuel consumption, and U is the cruise velocity. Because the natural logarithm of the mass ratio is inversely proportional to the L/D of the design, a low L/D can exponentially increase the fuel required to cover the same distance. Thus, for a high-speed cruise vehicle (such as a supersonic transport) to have any chance of economic success, attaining a high L/D should be an important objective.

For the case of a spaceplane, the same ideas apply – increasing the L/D of the vehicle will reduce the amount of fuel required to attain a specific orbit; this leads to more efficient operation of the vehicle. Higher efficiency corresponds to lower costs for putting payloads into orbit, thus making L/D important in spaceplane design.

1.2 Waveriders

One class of high-speed aerospace vehicles that have shown the ability to attain a high L/D compared to conventional designs is “waveriders.” A waverider is a supersonic or hypersonic vehicle in which a shock wave is attached along its entire leading edge; this attached shock wave keeps the high- and low-pressure fields distinctly separated, thus allowing the potential for a high L/D. Waveriders are usually designed inversely from a known supersonic or hypersonic flowfield (e.g., wedge or cone flow); an example of a cone-derived waverider is shown in Fig. 1.

1.3 Research Objectives

The use of Computational Fluid Dynamics (CFD) in modern aerospace research has shown many important applications. For example, necessary testing/experimentation can be reduced or eliminated, lowering overall development costs. Additionally, the ability of CFD to accurately predict the various properties and characteristics of a vehicle configuration can verify that the design is accurate, and determine whether modifications are required.

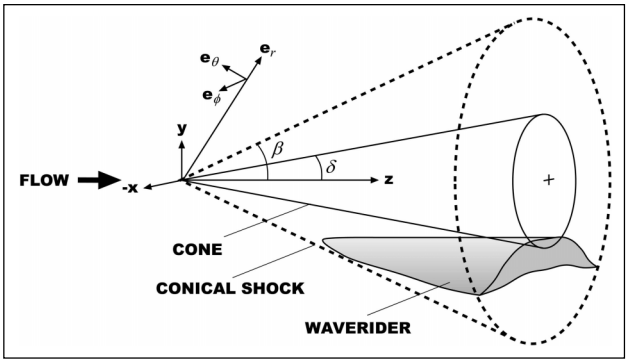

Fig. 1: Cone-Derived Waverider

Through the use of CFD, the flow around a waverider in supersonic or hypersonic flow can be accurately simulated. For this research, a Mach 3.5 design was numerically simulated to verify its waverider properties. Because this design will be used in a future supersonic wind-tunnel experiment, validation can ensure that the design is correct before embarking on an expensive model construction process. Table 1 shows the design conditions for the waverider used in this research (based on the characteristics of the wind-tunnel).

Mach Number	3.5
P_0 [atm]	5.0
T_0 [K]	293.0
Waverider Length [cm]	20.0

Table 1: Design Conditions

２．COMPUTATIONAL METHOD

2.1 Introduction

The computational method used in this research consists of several steps: 1) generation of the two-dimensional axisymmetric flow used to design the waverider, 2) design of the waverider from this generating flowfield, 3) construction of a three-dimensional finite-volume grid around the designed waverider, 4) solution of the three-dimensional Euler equations around the waverider configuration, and 5) calculation of the aerodynamic performance characteristics of the waverider.

2.2 Step 1: Obtaining a Generating Flowfield

The first step in designing a waverider is to obtain the generating flowfield. In much of the research relating to waveriders, conical flows are used. The Taylor-Maccoll equation expresses the analytical solution for supersonic conical flow; because this is only an ordinary differential equation, it can be

numerically integrated efficiently using techniques such as 4th-order Runge-Kutta methods.

Although this solution method is computationally fast, it limits waverider design to conical flowfields only. Thus, for this research, the CFD solution of the 2D axisymmetric Euler equations is used to obtain the generating flowfield for waverider design. [1] The algorithm used is the Beam-Warming method; time integration is performed implicitly (2nd-order temporal accuracy), and the fluxes are calculated using Yee's Symmetric TVD scheme (2nd-order spatial accuracy). Local time stepping is also used to accelerate convergence to steady-state.

For this research, the freestream conditions of the generating flowfield correspond to those in Table 1; the waverider was then designed from a conical flowfield (cone half-angle of 20 deg.) solved at these conditions.

2.3 Step 2: Waverider Construction

After the generating flowfield is obtained, the lower-surface base curve of the waverider is specified. This is performed by generating a series of cubic splines through 4 control points describing the base curve (see Fig. 2). From this base curve, the lower surface of the waverider is created by tracing the streamlines in the generating flowfield upstream until the shock wave is reached; this then determines the leading edge of the waverider. The upper surface of the waverider is then formed by tracing in the freestream direction from the leading edge to the base plane.

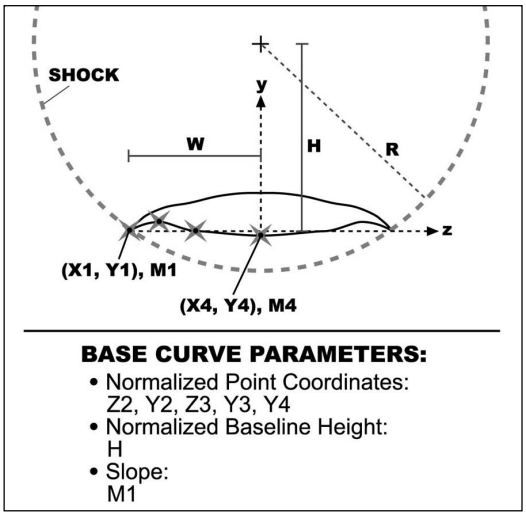

Fig. 2: Base Curve Parameters

Optimization is also used find the best waverider design from a given flowfield; in this process various parameters (including the aerodynamic characteristics) of the waverider are calculated. For the lift and drag calculations, the skin friction was estimated; thus the resulting design is viscous-optimized. Additionally, because a design suitable for a wind-tunnel experiment is desired, size and model-construction considerations have to be taken into account. Thus, for this research, the objective function:

$$F_{obj} = -\left(\frac{L}{D}\right)^a (\eta_{vol})^b (\theta_{edge})^c \left(\frac{l}{w}\right)^d, \quad \eta_{vol} = \frac{V^{2/3}}{A}, \qquad (2)$$

is minimized, where L/D is the lift/drag ratio, η_{vol} is the volumetric efficiency, θ_{edge} is the angle between the upper and lower surfaces at the leading edge, l and w are the waverider length and width, and V and A are the volume and surface area of the waverider, respectively. The constants a, b, c, and d determine the weight of each parameter in the optimization process; for this research a=7, b=1, c=4, and d=2 were used. Additionally, a constraint was implemented such that the design was required to allow a cylinder of a specified length and diameter fit inside the waverider. A length of 70.0 mm and diameter of 29.0 mm were used; this corresponds to the dimensions of the sting attachment mechanism that will be utilized for the wind-tunnel experiment. The optimization algorithm used is the Nelder-Mead downhill simplex method. [2]

2.4 Step 3: Grid Generation

In order to perform a three-dimensional CFD flow simulation of the waverider, finite-volume grids are constructed using an elliptic method. For this technique, the three-dimensional grid is first divided into a series of two-dimensional planes. Next, the boundaries of the grid in each plane are specified, and then the interior points are obtained by solving the two-dimensional Poisson equation, where the source term is a forcing function controlling the orthogonality of the grid at the body surface. Poisson's equation is solved using the line-SOR relaxation technique; further details regarding this algorithm can be found in Ref. [3].

For the specific grid used in this research, a series of two-dimensional planes was created normal to the flow direction (corresponding to cross-sections of the waverider). Because of narrow angle at the leading edge tip of the waverider in each plane, the upper and lower portions of the grid were divided into separate regions, and Poisson's equation was solved for each region. The dividing boundary between the two regions was selected to be parallel to the average of the upper and lower surface slopes at the leading edge. The points along the waverider surface were determined by interpolating the desired grid distribution onto the surface data generated during the design process.

For this research, a relatively coarse 46x36x26 grid (14,976 cells) was generated. Because the waverider is a symmetric design, only half of the configuration was simulated using CFD. The base plane and three-dimensional views of the grid are shown in Fig. 3 and 4, respectively. A close-up of the leading edge tip region is also shown in Fig. 3.

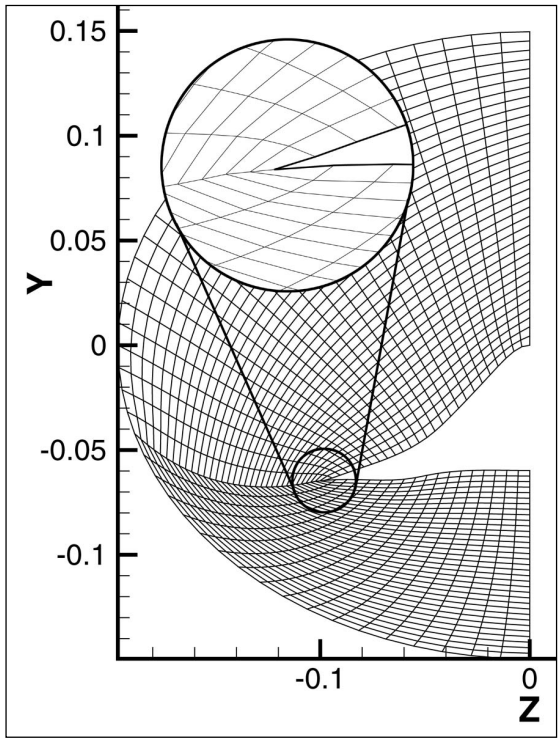

Fig. 3: Fine Grid Distribution in Base Plane

2.5 Step 4: CFD Method

In order to accurately validate the waverider properties of the design, a three-dimensional numerical simulation around half of the waverider configuration is performed. In conservation form, the three-dimensional Euler equations can be expressed in generalized coordinates as:

$$\frac{\partial \hat{U}}{\partial t} + \frac{\partial \hat{F}}{\partial \xi} + \frac{\partial \hat{G}}{\partial \eta} + \frac{\partial \hat{H}}{\partial \zeta} = 0,$$

$$\begin{aligned} \hat{U} &= U / J, \\ \hat{F} &= \left(\xi_x F + \xi_y G + \xi_z H\right) / J, \\ \hat{G} &= \left(\eta_x F + \eta_y G + \eta_z H\right) / J, \\ \hat{H} &= \left(\zeta_x F + \zeta_y G + \zeta_z H\right) / J, \end{aligned} \tag{3}$$

$$U = \begin{bmatrix} \rho \\ \rho u \\ \rho v \\ \rho w \\ e \end{bmatrix}, \quad F = \begin{bmatrix} \rho u \\ \rho u^2 + p \\ \rho uv \\ \rho uw \\ (e+p)u \end{bmatrix}, \quad G = \begin{bmatrix} \rho v \\ \rho vu \\ \rho v^2 + p \\ \rho vw \\ (e+p)v \end{bmatrix}, \quad H = \begin{bmatrix} \rho w \\ \rho wu \\ \rho wv \\ \rho w^2 + p \\ (e+p)w \end{bmatrix},$$

where the pressure is related to the other flow variables by the equation of state for a perfect gas. For this research, Eq. (3) is solved by performing ADI sweeps over the grid using the Beam-Warming algorithm. Time integration is performed implicitly using the two-point backwards Euler method (2nd-order temporal accuracy); the fluxes are calculated using Yee's Symmetric TVD scheme (2nd-order spatial accuracy). Local time stepping is used to accelerate convergence to steady-state. [4]

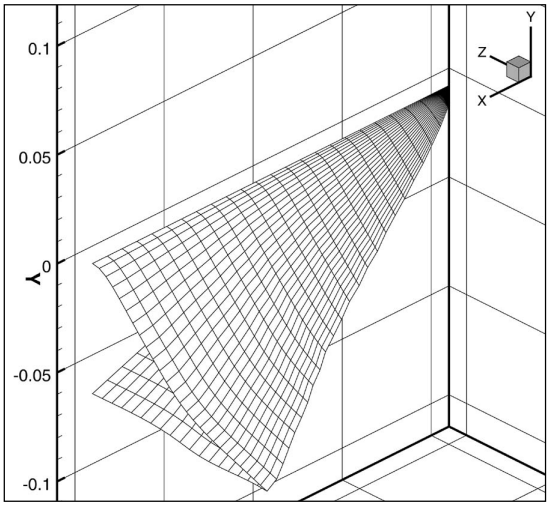

Fig. 4: Surface Grid Distribution (Half-Symmetric)

The boundary conditions are specified using a variety of techniques. Along the waverider surface, the velocity is determined from flow tangency. The surface pressure is obtained using second-order extrapolation, and the density is determined by assuming constant freestream enthalpy along the waverider surface. The inlet plane and outer-boundary are set to freestream conditions, and the exit plane is determined using zeroth-order extrapolation of the flow variables. [5]

2.6 Step 5: Aerodynamic Force Calculation

During the design process, the aerodynamic characteristics of the waverider are calculated by integrating the pressure forces over the surface (with the base plane assumed to be at freestream pressure). Viscous forces are included by using the reference temperature method to calculate the skin friction drag [6]; for this purpose, the design is assumed to have a fully turbulent boundary layer.

For the CFD flow simulation results, the same technique is used to obtain the performance characteristics of the waverider. The main difference between the two calculations is that the upper and lower surface pressure distributions are obtained from the three-dimensional results (rather than the generating flowfield). Because the base is not simulated, it is assumed to be at freestream pressure as in the design calculations; the skin friction on the waverider is also calculated using the same technique as in the design calculations.

3. RESULTS

Preliminary results were obtained from a coarse 46x36x26 grid. The base plane pressure contours of the waverider at steady-state are shown in Fig. 5; the left side corresponds to the CFD flow simulation, whereas the right side shows the design solution (i.e., the two-dimensional axisymmetric solution used to generate the waverider) interpolated onto the same grid.

For the coarse grid solution, it can be observed that although the shock wave location is somewhat different between the CFD and design results, the conical shock wave shape is still evident. Some leakage is also apparent near the leading edge of the waverider, although this may be partly due to the coarseness of the grid used.

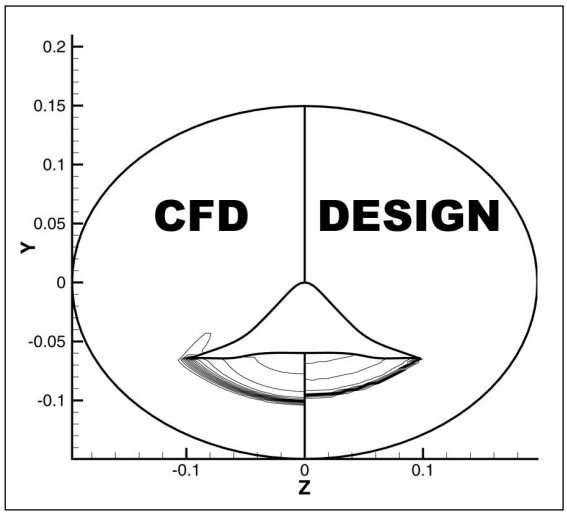

Fig. 5: Pressure Contours in Base Plane

A comparison of the aerodynamic characteristics of the waverider is presented in Table 2. Even though the grid utilized is very coarse, the C_L, and C_D of the two solutions are within 6% of each other, and the calculated L/D is less than 1% different.

	Design	*CFD*	*% Error of CFD*
C_L	0.085	0.090	5.8
C_D	0.024	0.025	4.2
L/D	3.53	3.52	-0.3

Table 2: Aerodynamic Characteristics

4. CONCLUSIONS

The three-dimensional Euler equations were successfully solved around a waverider. Through comparisons between the CFD solution and the design results, it was noted that although some differences were apparent in the flowfield structure, the aerodynamic characteristics of the different solutions were within close agreement. However, further numerical experiments using significantly finer grids are required for complete validation of the design. Additionally, viscous calculations (e.g., Navier-Stokes simulations) are also necessary to accurately model the viscous effects of the flow. Inclusion of the base plane flowfield might also yield more accurate results.

5. REFERENCES

(1) Lobbia, M. and Suzuki, K., "Design of Waveriders from Conical and Blunt-Body Flowfields," Proc. 22nd ISTS, ISTS-2000-e-07.

(2) Nelder, J. A., and Mead, R., "A Simplex Method for Function Minimization," Computer Journal, Vol. 7, pp. 308-313, 1965

(3) Hoffmann, K. A., Computational Fluid Dynamics for Engineers, Copyright ©1989, Engineering Education System

(4) Yee, H. C., "A Class of High-Resolution Explicit and Implicit

Shock-Capturing Methods," NASA TM-101088, Feb. 1989
(5) Pulliam, T. H., and Steger, J. L., "Recent Improvements In Efficiency, Accuracy, and Convergence for Implicit Approximate Factorization Algorithms," AIAA 85-0360, Jan. 1985
(6) Eckert, E. R. G., "Engineering Relations for Heat Transfer and Friction in High-Velocity Laminar and Turbulent Boundary-Layer Flow Over Surfaces with Constant Pressure and Temperature," Transactions of the American Society of Mechanical Engineers, Vol. 78, No. 6, 1956, pp. 1273-1283